pISSN 1229-3008 eISSN 2287-6251
Progress in Superconductivity and Cryogenics
Vol.20, No.4, (2018), pp.6~10 https://doi.org/10.9714/psac.2018.20.4.006

Correction of resonance frequency for RF amplifiers based on superconducting quantum interference device

Y. H. Lee[*,a], K. K. Yu[a], J. M. Kim[a], S. K. Lee[a], Y. Chong[b], S. J. Oh[c], and Y. K. Semertzidis[c]

[a] *Ultra-low Magnetic Field Team, Korea Research Institute of Standards and Science, Daejeon, Korea*
[b] *Quantum Information Team, Korea Research Institute of Standards and Science, Daejeon, Korea*
[c] *Center for Axion and Precision Physics Research, Institute for Basic Science, Daejeon, Korea*

(Received 22 December 2018; revised or reviewed 29 December 2018; accepted 30 December 2018)

Abstract

Low-noise amplifiers in the radio-frequency (RF) band based on the direct current (DC) superconducting quantum interference device (SQUID) can be used for quantum-limited measurements in precision physics experiments. For the prediction of peak-gain frequency of these amplifiers, we need a reliable design formula for the resonance frequency of the microstrip circuit. We improved the formula for the resonance frequency, determined by parameters of the DC SQUID and the input coil, and compared the design values with experimental values. The proposed formula showed much accurate results than the conventional formula. Minor deviation of the experimental results from the theory can be corrected by using the measured geometrical parameters of the input coil line.

Keywords: SQUID, radio-frequency amplifier, resonance frequency, amplification gain

1. INTRODUCTION

Quantum-noise-limited amplifiers in the radio-frequency (RF) range are attracting attention recently for application to precision physics experiments, for example, detection of axion-mediated weak RF signals from a cryogenic microwave cavity [1] and Qubit experiment in quantum information processing [2]. RF amplifier based on superconducting quantum interference device (SQUID) has advantage that it has wide bandwidth and moderate gain at its peak-gain frequency [3, 4].

The resonance frequency or peak-gain frequency of these amplifiers is mainly determined by input coil parameters of the SQUID, such as input coil linewidth and thickness of the insulation layer between the input coil and the SQUID loop, where the input coil is formed on the SQUID loop in the form of microstrip line. The conventional formula for the resonance frequency agrees well with the experimental data below about 100 MHz. Table 1 shows some fabricated RF amplifiers, with resonance frequency in the range of 105 MHz to 2.65 GHz [4]. The deviation between the measured resonance frequency f_0 and calculated frequencies ($f_0^{\mathrm{calc}}(L_0)$ and $f_0^{\mathrm{calc}}(n^2L)$) using two different formulas increases much as the frequency increases, making it difficult to predict the resonance frequency in the design stage. And the two calculation results are also quite different each other.

For axion search experiments, we need RF amplifiers with resonance frequency around 1 GHz and above. Thus we need a more exact formula for the resonance frequency.

* Corresponding author: yhlee@kriss.re.kr

We have been developing SQUID-based RF amplifiers with an aiming to be used for axion-mediated RF signals, and found that the resonance frequency can be predicted well if the formula is modified to consider the stray inductance of the SQUID loop. We designed and fabricated several structures of SQUID-based RF amplifiers, and compared the experimental results with the theory.

TABLE 1
MEASURED AND CALCULATED RESONANCE FREQUENCY FOR SIX MICROSTRIP SQUID AMPLIFIERS WITH DIFFERENT SQUID INDUCTANCE L AND INPUT COIL TURNS N. MODIFIED FROM [4].

SQUID	L (pH)	n	ℓ (mm)	f_0 (MHz)	$f_0^{\mathrm{calc}}(L_0)$ (MHz)	$f_0^{\mathrm{calc}}(n^2L)$ (MHz)
1	350	40	98	105	500	91
2	350	15	23	370	2100	500
3	350	11	16	590	3000	820
4	350	6	8	1200	6200	2200
5	90	8	4	2200	12330	4400
6	90	7	3	2650	15000	5300

f_0: measured frequency, $f_0^{\mathrm{calc}}(L_0)$: calculated using microstrip model, $f_0^{\mathrm{calc}}(n^2L)$: calculated using multi-turn input coil model.

2. RESONANCE FREQUENCY MODEL

2.1. Basic configuration of SQUID RF amplifier

SQUID is a transducer from magnetic flux to voltage, where the input signal is a physical quantity which can be converted to the form of magnetic flux. To increase the signal coupling between the input coil and the SQUID loop, a multiturn input coil is used. The multiturn input coil then

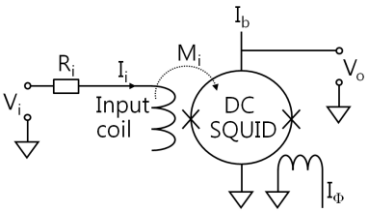

Fig. 1. Structure of the SQUID-based RF amplifier. One end of the input coil is left open, and the RF signal is applied to the other end of the input coil and the ground. Input RF signal V_i applied to the input coil generates current in the input coil which is converted to magnetic flux via mutual inductance M_i. To adjust the flux bias in the SQUID, DC current I_Φ is applied to the SQUID.

introduces parasitic capacitance between the input coil and the SQUID loop, resulting in loss of RF power during signal transmission. One way of circumventing the parasitic capacitance effect is to use this capacitance to form a RF transmission structure where the input coil and SQUID loop forms a microstrip transmission line. Here, one end of the input coil should be left open to form a half-wavelength resonator and the input signal is applied between the other end of the input coil and ground, as shown in Fig. 1 [4-6]. This type of amplifier is also called microstrip SQUID amplifier (MSA).

2.2. Resonance frequency of SQUID RF Amplifier

2.2.1. Microstrip resonance model

In the superconducting microstrip conductor, the multiturn input coil is separated from SQUID loop by a dielectric layer of thickness d and dielectric constant ε.

The multiturn input coil has a linewidth w. Assuming that the thickness of two superconducting films are sufficiently thicker than the London penetration depth of the superconductor λ and $w>>d$, the capacitance and inductance per unit length of the microstrip are respectively given as following [4],

$$C_0=\varepsilon\varepsilon_0 w/d \quad \text{(F/m)}, \tag{1}$$

$$L_0=(\mu_0 d/w)(1+2\lambda/d) \quad \text{(H/m)}, \tag{2}$$

where, ε_0 and μ_0 are permittivity and permeability in vacuum. The velocity of an electromagnetic wave in the microstrip is then given by

$$c^*=1/(L_0C_0)^{1/2}=c/[\varepsilon(1+2\lambda/d)]^{1/2}, \tag{3}$$

where, c is the velocity of light in vacuum. Finally the characteristic line impedance of the microstrip is given by

$$Z_0=(L_0/C_0)^{1/2}=(d/w)[\mu_0(1+2\lambda/d)/\varepsilon\varepsilon_0]^{1/2}. \tag{4}$$

When the microstrip has length l, and its ends are open, it becomes a half-wave resonator with its wavelength given by the relation, $l=\lambda_0/2$, with λ_0 being the resonance wavelength.

Then, the resonance frequency $f_0(L_0)$ of the microstrip is given by,

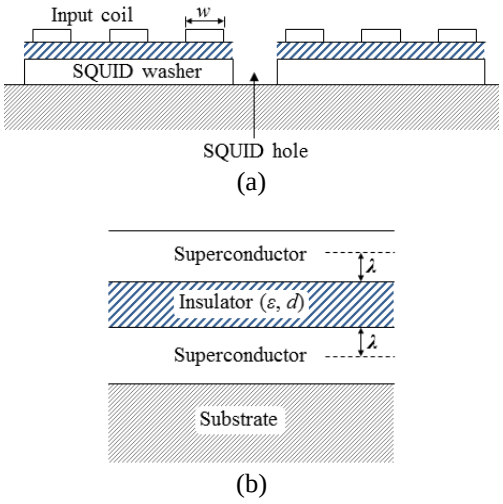

Fig. 2. Cross-sectional view of the microstrip line. (a) Multiturn input coil is separated by a dielectric layer from the SQUID washer. (a) Side view showing the vertical structure.

$$f_0(L_0)=c^*/\lambda_0=c^*/2l=1/2l(L_0C_0)^{1/2}=c/2l(\varepsilon(1+2\lambda/d))^{1/2}. \tag{5}$$

When the resonance frequency is below about 100 MHz, The expression (Eq. 5) agrees reasonably well with the experimental results. If the frequency increases, however, Eq. (5) starts to deviate from the measured ones. For example, at 2.2 GHz, measured one is about 5.6 times smaller than that ($f_0^{\text{calc}}(L_0)$) given by Eq. (5) as shown in Table 1, mainly due to contribution of the parasitic inductance in the wiring of RF input lines [4].

2.2.2. Multi-turn input coil model

Since RF signal is coupled into the SQUID loop via tightly wound multi-turn input coil, the inductance of the input coil can be treated the same way as the near-DC signal coupling, so called Ketchen type coupling [7]. Taking this input coil inductance in the calculation of the resonance frequency, it can be written by,

$$f_0(n^2L_{SQ})=c^*/2l=1/2l(L_0^*C_0)^{1/2}=1/2n(lL_{SQ}C_0)^{1/2}, \tag{6}$$

where, $L_0^*=L_i/l=n^2L_{SQ}/l$ is inductance of the input coil per unit length, l input coil length, n number of input coil turn, L_i input coil inductance and L_{SQ} SQUID inductance. Calculated values by Eq. (6) were about 2 times larger than measured ones in the GHz range, as shown in Table 1 [4].

2.2.3. Modification of multi-turn input coil model

In the near-DC application of the SQUID, the SQUID hole size (and its inductance) is typically large to have large input coil inductance, necessary for inductance matching with the pickup coil. Thus SQUID hole inductance is the major part of the SQUID inductance, that is, the contribution of slit inductance is negligible. In the high frequency range for RF amplifier application, the SQUID hole size should be smaller. Then the contribution of the slit inductance should be included in the calculation of total

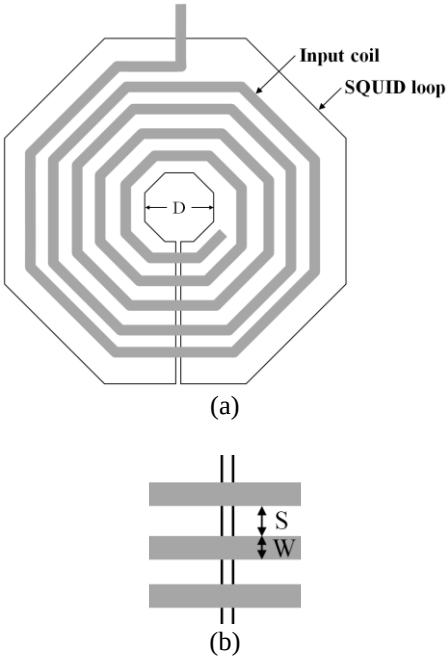

Fig. 3. Structure of SQUID loop and input coil. (a) Octagonal SQUID washer and multi-turn octagonal coil. (b) Linewidth (w) and space (s) of the input coil line.

SQUID inductance. The slit inductance is experimentally given as roughly 0.3 pH/μm, if there is no ground plane under the slit [7].

Here we use a modified formula for the SQUID inductance including the stray inductance of the slit,

$$L_{SQ}=L_h+(n\cdot(w+s)\ \mu\text{m})\cdot 0.3\ \text{pH/}\mu\text{m}, \quad (7)$$

where L_h is SQUID hole inductance, n is number of turns of the input coil, w and s are linewidth and space of the input coil line, respectively.

Inductance of SQUID hole with an octagonal washer L_h is given by $1.05\mu_0 D$, with D the inner dimension of the washer, as shown in Fig. 3. For comparison, the square washer has inductance of $1.25\mu_0 D$. That is, octagonal washer has smaller inductance than that of square washer, allowing more turn in the input coil winding, and is more suitable for high frequency operation. Furthermore, the input line bends 45 degree at each corner, providing more smooth transmission of RF signal along the input coil.

Figure 4 shows the design pattern of the RF amplifier. The RF signal is coupled into the SQUID loop through the taped bonding pad (RF in) and spiral input coil integrated on top of the SQUID washer. DC current bias and RF output measurement were done through the RF out pad. In the RF input pad, a coupling capacitor was used. This capacitor has effect on the bandwidth of the gain curve; larger coupling capacitor broadens the gain curve at the expense of slightly reduced peak gain compared with the optimum capacitance for critical coupling [8].

We designed SQUID amplifiers of different input coil parameters; linewidth and space of input coil line, number of turn. Table 2-4 shows the summary of SQUID parameters for 3 types of SQUID design. All the SQUIDs have the same SQUID hole dimension of 20 μm, and dielectric constant of SiO_2 was assumed to be 4.5.

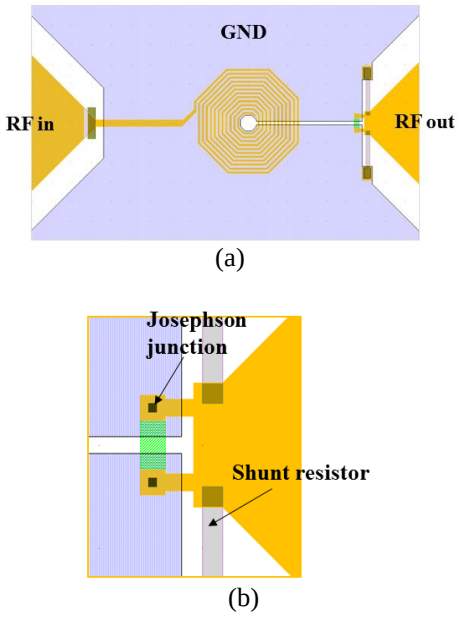

Fig. 4. Design of SQUID amplifier. (a) Whole SQUID layout. (b) Details of the design around the Josephson junction area.

TABLE 2
SQUID PARAMETERS FOR TYPE-A RESONATOR.

Parameter	Figure	Unit
Input coil width	4.0	μm
Input coil space	3.0	μm
SiO_2 insulator thickness	0.275	μm
Specific capacitance C_0	5.80×10^{-10}	F/m
Specific inductance L_0	1.81×10^{-7}	H/m

TABLE 3
SQUID PARAMETERS FOR TYPE-B RESONATOR.

Parameter	Figure	Unit
Input coil width	8.0	μm
Input coil space	3.0	μm
SiO_2 insulator thickness	0.275	μm
Specific capacitance C_0	1.16×10^{-9}	F/m
Specific inductance L_0	9.03×10^{-8}	H/m

TABLE 4
SQUID PARAMETERS FOR TYPE-C RESONATOR

Parameter	Figure	Unit
Input coil width	2.0	μm
Input coil space	2.0	μm
SiO_2 insulator thickness	0.275	μm
Specific capacitance C_0	2.29×10^{-10}	F/m
Specific inductance L_0	3.61×10^{-7}	H/m

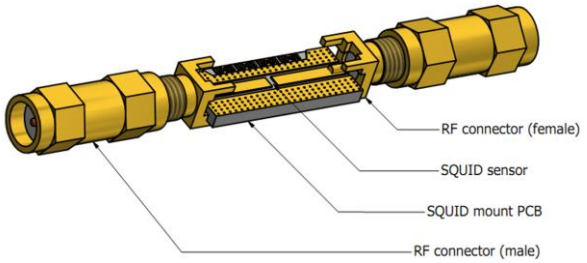

Fig. 5. Package for SQUID mounting.

3. FABRICATION OF SQUIDS

3.1. Fabrication process of SQUID amplifiers

SQUID chips were fabricated using optical lithography and Nb/AlO_x/Nb multilayer thin film process. The superconducting material used is Nb having critical temperature of about 9 K, and can be operated reliably at 4.2 K, the temperature of liquid He. Josephson junction fabricated with Nb has low sub-gap leakage current and has been used in low-noise SQUIDs. Especially, Nb is a refractory metal and is physically very stable against repeated thermal between room temperature and low temperature. Furthermore, multilayer integration using semiconductor fabrication process is possible. The fabrication process consists of 5 depositions (Nb/AlO_x/Nb, SiO_2-1, SiO_2-2, Pd and Nb), 1 dry etching using reactive ion etching for defining Josephson junctions, 4 lift-off processes, and 5 photo-lithography process [9]. Size of each Josephson junction is 2 μm × 2 μm. Fig. 5 shows the package for the SQUID [10].

4. MEASUREMENT OF AMPLIFIER GAIN CURVE

4.1. Measurement setup

Since SQUID amplifier is a very sensitive detector, its output can be saturated easily even at low input RF power. In order to apply low input power, we decreased the output power of the network analyzer (Agilent Technologies, model E5071C) to its minimum level, -55 dBm. And then we used two 40-dB attenuators, one at room temperature and the other one at 4.2 K. Fig. 6 shows the schematic diagram of the gain measurement set up.

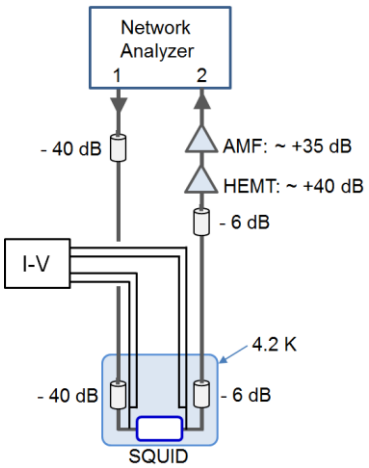

Fig. 6. Schematic diagram of the measurement setup.

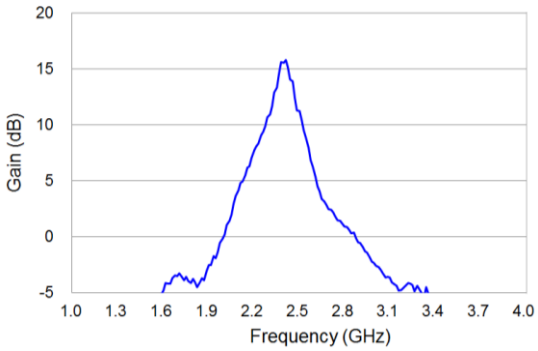

Fig. 7. Gain curve of a SQUID amplifier.

Before we decide the working point, we checked the current-voltage curves of the SQUID while changing the magnetic flux, and then we fixed the bias current to provide near maximum flux modulation voltage. The flux bias point is near $\Phi_0/4$ (Φ_0: flux quantum), where the flux-to-voltage transfer is near the maximum. The output of SQUID was amplified by room temperature semiconductor amplifiers with altogether gain of about 75 dB. Between SQUID and room temperature amplifiers, we put two 6-dB attenuators, one at room temp and one at 4.2 K, to avoid penetration of thermal noise into the SQUID.

4.2. Measured gain curve

One example of the gain curve is shown in Fig. 7. The resonance frequency is near 2.4 GHz, with peak gain of about 16 dB.

4.3. Dependence of resonance frequencies on the input coil parameters

Figs. 8-10 show the gain peak frequencies for 3 types of resonator: type-A, -B, and -C. The measured peak-gain frequencies agree reasonably well with the calculated values using the modified model described in Section 2.2.3. But some deviation was found between the measured and calculated ones.

After measuring the real linewidth and space dimensions of the input coils using an optical microscopy from the fabricated SQUIDs, we recalculated the resonance frequencies.

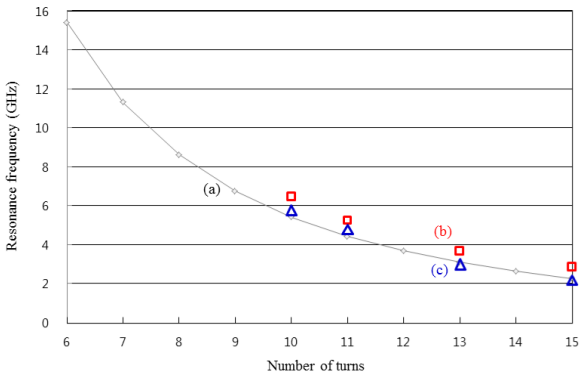

Fig. 8. Resonance frequency vs. number of input coil turn in type-A resonator. (a) Calculated for input coil with 4 μm linewidth and 3 μm space (○), (b) measured frequency (□), and (c) recalculated frequency using the measured linewidth and space dimensions (Δ).

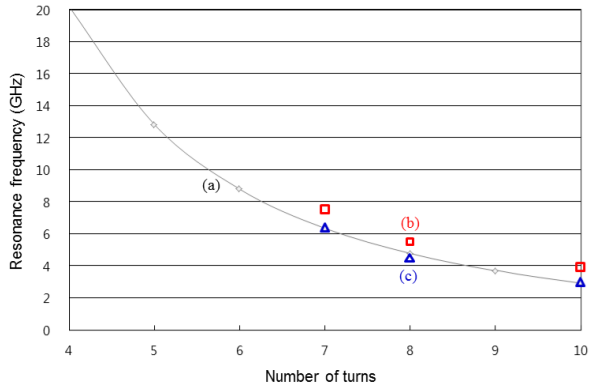

Fig. 9. Resonance frequency vs. number of input coil turns in type-B resonator. (a) Calculated for input coil with 8 μm linewidth and 3 μm space (○), (b) measured frequency (□), and (c) recalculated frequency using the measured linewidth and space dimensions (Δ).

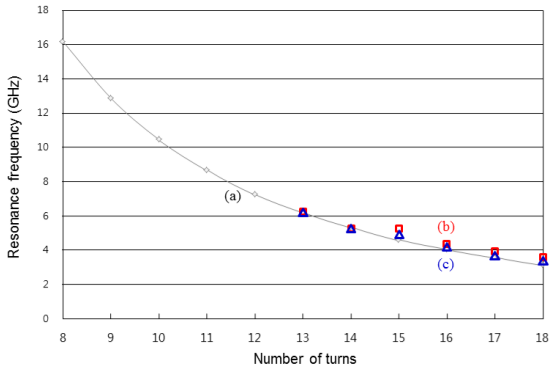

Fig. 10. Resonance frequency vs. number of input coil turns in type-C resonator. (a) Calculated for input coil with 2 μm linewidth and 2 μm space (○), (b) measured frequency (□), and (c) recalculated frequency using the measured linewidth and space dimensions (Δ).

Then, the agreement between the measured and recalculated ones becomes better, as shown in the Figs. 8-10. This means that the input coil model predicts the resonance frequency quite accurately if the SQUID inductance is correctly calculated, and linewidth and space of the input coil is exactly known.

5. CONCLUSIONS

The multi-turn input coil model, with stray inductance of the slit structure included in the SQUID inductance, predicts the peak-gain frequency of the RF amplifier with acceptable accuracy. Some difference between the calculated frequencies and measured ones seems to be from the mismatch in the material parameters, that is, linewidth of the input coil line, thickness and dielectric constant of the dielectric layer. If the measured dimensions of the input coil line were used to calculate the resonance frequencies, the agreement with the measured ones improved, meaning that the multi-turn input coil model with correct SQUID inductance value can predict the resonance frequency of the SQUID-based RF amplifier within 10-20% accuracy.

ACKNOWLEDGMENT

This work was supported by IBS project of CAPP (IBS-R017-D1-2018-a01).

REFERENCES

[1] S. J. Asztalos et al., “Design and performance of the ADMX SQUID-based microwave receiver”, *Nucl. Instr. Meth. Phys. Res. A*, 656, pp. 39-44, 2011.

[2] S. Michotte, “Qubit dispersive readout scheme with a microstrip superconducting quantum interference device amplifier”, *Appl. Phys. Lett.*, 94, pp. 122512-1~3, 2009.

[3] Y. H. Lee, Y. Chong and Y. K. Semertzidis, “Review of low-noise radio-frequency amplifiers based on superconducting quantum interference device”, *Prog. Supercond. Cryog.*, 16, pp. 1-6, 2014.

[4] J. Clarke, A. T. Lee, M. Mück and P. L. Richards, “SQUID Voltmeters and Amplifiers”, p. 22-115, Chap. 8, in *The SQUID Handbook*, Eds. J. Clarke and A. I. Braginski, 2006, Wiley-VCH.

[5] J. Clarke, M. Mück, M. André, J. Gain and C. Heiden, “The Microstrip DC SQUID Amplifier”, p. 473-504, in *Microwave Superconductivity*, Eds. H. Weinstock and M. Nisenoff, 2001, Kluwer Academic Pub.

[6] M. Mück, and J. Clarke, “The superconducting quantum interference device microstrip amplifier: Computer models”, *J. Appl. Phys.*, 88, pp. 6910-6918. 2000.

[7] M. B. Ketchen, “Integrated thin-film dc SUIDs sensors”, *IEEE Trans. Magn.*, Mag-23, pp. 1650-1657, 1987.

[8] D. Kinion and J. Clarke, “Microstrip superconducting quantum interference device radio-frequency amplifier: Scattering parameters and input coupling”, *Appl. Phys. Lett.*, 92, 172503, 2008.

[9] Y. H. Lee, J. M. Kim, K. Kim, H. Kwon, K. K. Yu, I. S. Kim and Y. K. Park, “64-channel magnetocardiogram system based on double relaxation oscillation SQUID planar gradiometers”, *Supercond. Sci. Technol.*, 19, pp. S284-S288, 2006.

[10] Y. H. Lee et al., “Development of SQUID-based high-frequency quantum amplifiers”, Annual Report, IBS (IBS-R017-D1-2014-a01), 2015.